Kink Bands in Form II of Syndiotactic Polypropylene

Finizia Auriemma,* Claudio De Rosa, Odda Ruiz de Ballesteros, and Paolo Corradini

Dipartimento di Chimica, Università degli Studi di Napoli Federico II, via Mezzocannone 4, 80134 Napoli, Italy

Received March 4, 1997; Revised Manuscript Received June 22, 1997[⊗]

ABSTRACT: Samples of highly syndiotactic polypropylene (s-PP), when quench precipitated from solution, have an X-ray diffraction spectrum close to that calculated for the limit-ordered $C222_1$ form II of s-PP. The solid state ^{13}C NMR CP MAS spectrum shows, however, evidences of the presence of a significant amount (≈20%) of long portions of chains in *trans* planar conformation $(TT)_n$ immobilized between crystal regions with chains in $(TTGG)_n$ conformation. It is shown that form II of s-PP is geometrically suitable for the formation of kink bands, in which portions of chains in *trans* planar conformation are embedded: atomic coordinates can be deduced for a simplified statistical model of disordered crystal assumed to be periodic in the two directions perpendicular to the (TTGG) helical stretches. All *gauche* bonds have the same sign (G_+ or G_-) in the disordered crystal. Formulas may be written for the calculation of the X-ray diffraction of such crystals. The X-ray diffraction pattern calculated for a set of small, partially disordered $C222_1$ crystals comprising portions of chains which have statistically approximately six consecutive *trans* bonds in the kink bands every 20−30 monomeric units, as in the ratio indicated by the NMR spectra, is in good agreement with the experimental pattern.

Introduction

Kink bands were firstly described in metals and salt crystals and have been observed in semicrystalline and amorphous oriented polymeric samples as well (see for instance ref 1, pp 497−498 and references therein). The kink bands are a type of deformation band which can be created by compressive stress parallel to the *c* axis direction in macromolecular crystals, (i.e. the crystallographic axis usually taken parallel to the chain axis) and involve a change in neighboring chains of the chain axis direction. They have been observed, for instance, in the electron microphotograph of extended chain crystals of poly(tetrafluoroethylene),[2,3] polyethylene,[4] and α-nylon[5,6] as a result of defective crystal growth or deformation (see also ref 1, p 466). More recently detailed structural X-ray diffraction studies on poly (vinylidene fluoride) have evidenced the presence of kink bands in the polymorphs named form I and form II.[7,8] They consist in the presence in the crystallites of portion of chains assuming a conformation different from the conformation of the limit-ordered form. The defects, which concern groups of neighboring chains, have the property of deviating locally the chain axis direction but still preserving the parallelism among chain axes and extend over wide regions of the crystallites.

Kink bands have been also postulated in our preceding papers in the case of syndiotactic polypropylene (s-PP)[9,10] in order to explain the solid state ^{13}C NMR CP MAS spectra of highly disordered s-PP samples (quench precipitated from the solution) showing structural features close to those calculated for the "ideal" C-centered orthorhombic structural model of s-PP (form II after ref 11). The solid state ^{13}C NMR CP MAS spectra of such s-PP samples present, indeed, additional resonances besides those expected in the case of the limit-ordered form II with chains in fully helical $(TTGG)_n$ conformation, belonging to nuclei placed in well defined conformational environments embedded in rigid structures. In ref 9 some possible structural models of s-PP in this disordered form were drawn: the proposed models comprise defective but energetically feasible portions of chains in *trans*-planar conformation (disturbing the dominating $(TTGG)_n$ conformation); the last are imagined to be clustered on planes which cross the 3D otherwise ordered portions of the crystallites and form kink bands.

We recall that the most stable form of s-PP (form I) found by Lotz, Lovinger, et al.[12] also presents disorder phenomena. They are related to packing rather than to conformational defects[13−16] and indeed, solid state ^{13}C NMR spectra of s-PP samples crystallized in form I present only resonances typical of $(TTGG)_n$ helical conformation.[9,10,17]

It is worth noting that another polymorph of s-PP, form IV after ref 11, with chains in a $(T_6G_2T_2G_2)_n$[18] conformation, presents spectral features analogous to those of the quench-precipitated sample of s-PP of ref 9, in the ^{13}C NMR CP MAS spectrum.[19] In refs 9 and 10, we already excluded that the quench-precipitated s-PP samples would be prevailingly in form IV, based on (i) the different positions of the Bragg reflections in form II and form IV and (ii) the different thermal behavior of the two kinds of samples. As described in detail in ref 10, the ^{13}C NMR CP MAS spectra of the quench-precipitated s-PP sample obtained at different temperatures do not present substantial differences up to 100 °C; the extra resonances disappear completely only upon the melting (i.e. above 140 °C). For form IV, instead, it is known from the literature[18] that it transforms to the more common crystalline form with chains in the $(TTGG)_n$ fully helical conformation on heating the sample at T ≥ 50 °C, already.

As outlined in ref 20, the disordered model structures proposed for the quench-precipitated s-PP samples in ref 9 may be considered intermediate between the limit-ordered models of form II and form IV: corresponding to the kink bands, the chains assume a conformation as well as a packing mode close to those of form IV. This explains the analogy of the ^{13}C NMR CP MAS spectra of samples in form IV and in the disordered form II containing kink bands. A detailed structural analysis of the aforementioned disordered structure of s-PP involving kink bands has not yet been performed so far.

[⊗] Abstract published in *Advance ACS Abstracts,* August 15, 1997.

S0024-9297(97)00284-2 CCC: $14.00

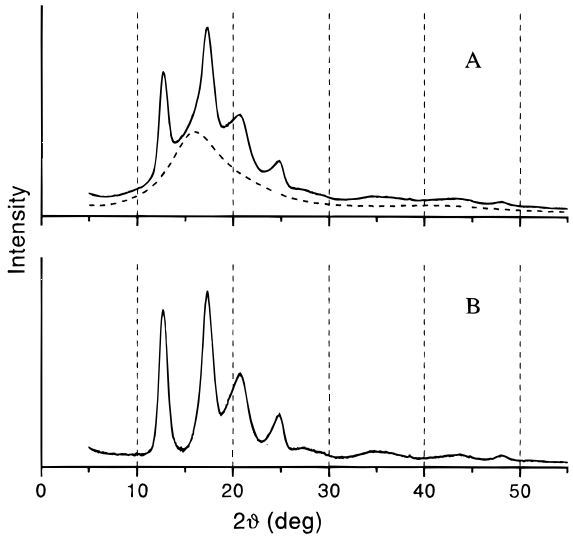

Figure 1. X-ray powder diffraction profiles of the quench-precipitated s-PP sample (solid line) before (A) and after the subtraction of the amorphous contribution (B). The dashed line in part A indicates the amorphous halo.

In this paper, the X-ray diffraction profiles of ordered as well as of disordered trial model structures comprising kink bands are calculated, and the results of the calculations are compared with the experimental X-ray diffraction profile of a s-PP sample in the disordered form II.

It is worth noting that in ref 9 we discussed also another kind of conformational disorder in form II of s-PP arising from the presence along the same chain of inversion in the sense of spiralization of the helices. This kind of disorder would imply statistical substitution of right- and left-handed helices in the lattice positions. This disorder would affect the intensity of ($h0l$) reflections with $l = 2n + 1$ in the limit-ordered structure of form II.[21] Since (110) and (201) reflections contribute the same amount to the maximum at $2\theta = 17°$ in the Cu Kα X-ray powder diffraction pattern,[22] the presence of disorder due to the random substitution of right- and left-handed helices in the lattice positions would decrease the intensity maximum at $2\theta = 17°$, against any experimental evidence for our sample and will not be investigated here. As discussed in ref 21, this disorder is probably present in fiber specimens of s-PP and/or in less stereoregular s-PP samples crystallized in form II (see also ref 9).

Experimental Section

The s-PP sample was supplied by "Montell". The polymer was synthesized with a syndiospecific homogeneous catalyst based on a column 4 (group 4A) metallocene/methylaluminoxane system according to the procedure explained in ref 23. The studied sample ($M_w = 120 \times 10^3$) was obtained by performing the polymerization at 44 °C. It is highly syndiotactic with a content of fully syndiotactic pentads (*rrrr*) equal to 86%. It corresponds to the same (quench-precipitated) s-PP sample of refs 9 and 10 (sample A) whose solid state ^{13}C -NMR spectrum has been already described in the Introduction.

X-ray powder diffraction spectra were recorded at room temperature with a Philips powder diffractometer using Ni-filtered Cu Kα radiation and a step scan procedure. The range of 2θ diffraction angle examined was 5−55°, the count time for each step was equal to 60 s/step, and the step was 0.04° (2θ).

The X-ray powder diffraction pattern of our s-PP sample is reported in Figure 1A (solid line). The X-ray diffraction profile of an amorphous polypropylene sample suitably scaled on the intensity scale is also reported (dashed line). The diffraction profile of s-PP after the subtraction of the amorphous contribution is reported in Figure 1B.

There are four most intense reflections, located at $d = 7.20$ Å ($2\theta = 12.3°$, Miller indices (200)), $d = 5.22$ Å ($2\theta = 17.0°$, Miller indices (110) + (201)), $d = 4.29$ Å ($2\theta = 20.7°$, Miller indices (111)), and $d = 3.63$ Å ($2\theta = 24.5°$, Miller indices (002) + (400) + (310)). The presence of a reflection centered at $d = 5.22$ Å ($2\theta = 17.0$ °) and the absence of the reflection centered at $d = 5.70$ Å ($2\theta = 15.8°$) indicate that this sample is crystallized in a form very close to the form II of s-PP; i.e. the unit cell is *C* pseudo-centered.[24] The 2θ positions of the reflection peaks are compatible with an orthorhombic unit cell with constants very close to those proposed for the form II of s-PP in refs 22 and 24 ($a = 14.5$ Å, $b = 5.60$ Å and $c = 7.40$ Å).

Model Structures for Trial Calculations

As resumed in the introduction, the disorder which can possibly account for the ^{13}C-NMR CP MAS spectra and the X-ray diffraction profiles of the sample under study is of conformational origin: portions of chains in *trans*-planar conformation are possibly included in chains in the prevailing TTGG conformation, without disturbing the packing of s-PP in form II.

We recall that form II of s-PP is characterized by an isochiral packing of helices.[22,24] It may be described in terms of an orthorhombic unit cell centered on the *C*-face with axes $a_o = 14.50$ Å, $b_o = 5.60$ Å, and $c_o = 7.40$ Å, space group $C222_1$. The packing models in the $a-c$ and $a-b$ projections are shown in Figures 2A and 3A, respectively.

It is known, on the other hand, that s-PP may crystallize under special conditions in form IV, with chains in a $T_6G_2T_2G_2$ conformation, which is somehow intermediate between the *trans*-planar and the TTGG helical conformation. It was originally proposed for form IV of s-PP a triclinic unit cell (space group $P1$[18]). We have recently shown that form IV of s-PP may be likewise described, upon small changes of the atomic coordinates, in terms of a monoclinic structural model (space group $C2$) with the cell, centered on the *C* face, having axes $a_m = 14.14$ Å, $b_m = 5.72$ Å, $c_m = 11.6$ Å, and $\beta = 108.8°$.[20] The latter would be better suited as being descriptive of the long-range limit-ordered structure, whereas the validity of the triclinic structural model remains for the description of local situations of order. The packing models of s-PP in the form IV according to the monoclinic description, in the $a-c$ and $a-b$ projections, are shown in Figures 2D and 3B respectively.

As outlined in ref 20 the monoclinic structural model for s-PP in form IV presents many similarities with the orthorhombic structural model for s-PP in form II (compare Figure 2A with Figure 2D and Figure 3A with Figure 3B): (i) they both are *C*-centered; (ii) they both correspond to an isochiral packing of helices; (iii) they are nearly isometric as far as the *a* and *b* unit cell dimensions; (iv) the length of the projection of the c_m axis in the direction perpendicular to the $a-b$ plane ($c_m \sin \beta$) corresponds to nearly $^3/_2c_o$.

Within this frame the model structures proposed in ref 9 for s-PP in the highly disordered form II appear, somehow, as possible examples of intermediate structures between the limit-ordered structural models proposed for form II and form IV. One of these model structures is re-drawn from ref 9 in Figure 2B whereas in Figure 2C another possible model structure, also compatible with the experimental ^{13}C NMR CP MAS data, is shown, as an example. They are characterized by portions of chains in the helical conformation (TTGG), all having the same chirality, located at the top and at the bottom of the structural models of Figure 2B,C.

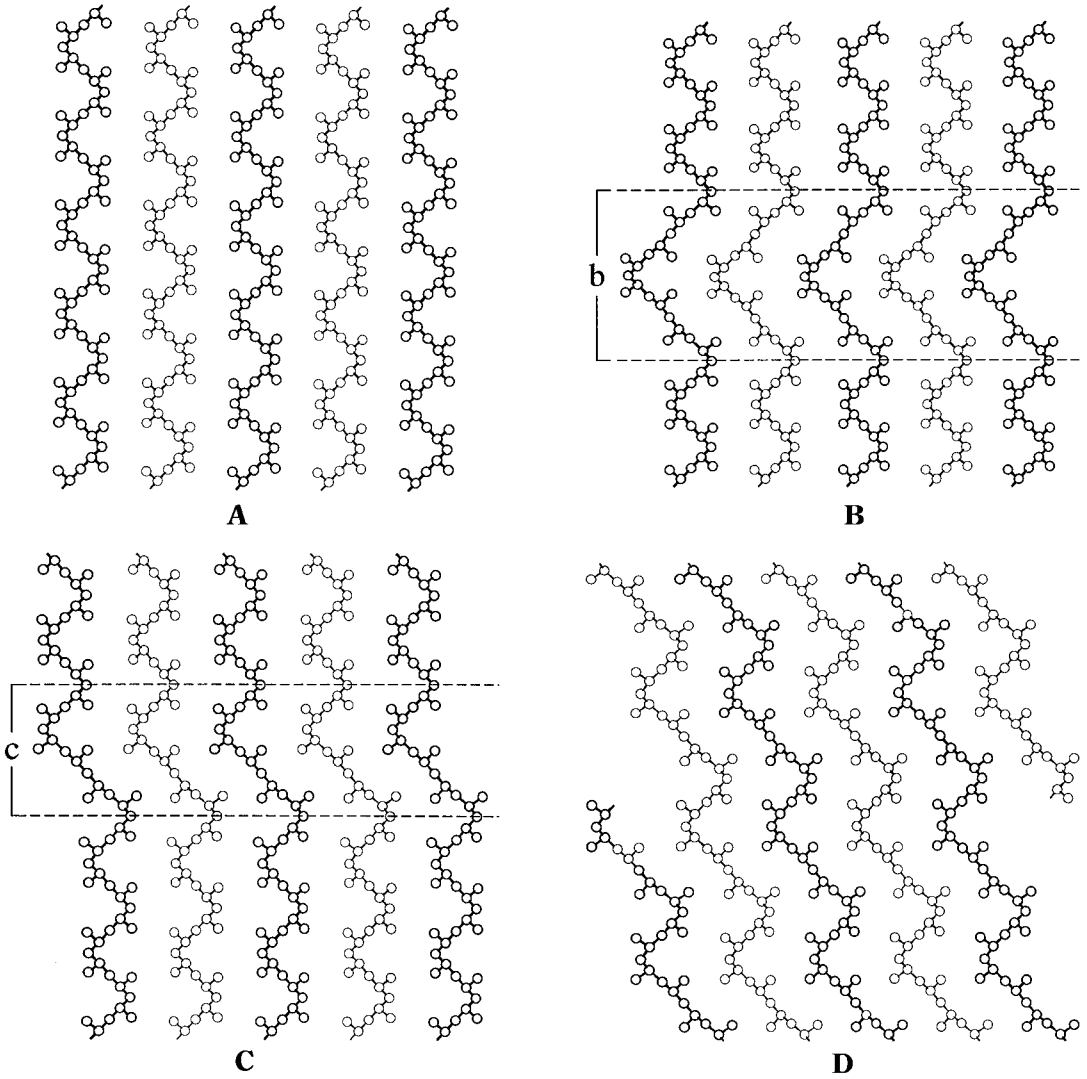

Figure 2. $a-c$ projection of the limit-ordered structural model of form II of s-PP (space group $C222_1$) (A) and of form IV of s-PP (space group $C2$) (D) and two examples of disordered intermediate structural models (B,C). Chains drawn with thin and bold lines are at 0 and $^1/_2$ along b (perpendicular to the plane of drawing). In B and C the regular portions of the crystals have chains in the (TTGG) conformation like in A. The "defective" portions of the chains in B correspond to a conformational sequence $G_2T_6G_2T_6$ (portion b); the defective portions of the chains in C, corresponds to the conformational sequences $G_2T_{2(2n+1)}$ with $n = 1$ (portion c). At the boundary between the regular and the defective portions of the crystal, local packing situations similar to those of D occur.

These portions of chains are packed according to the limit-ordered structural model of form II, (space group $C222_1$) and are connected by portions of chains in $T_6G_2T_6G_2$ conformation (Figure 2B, b portion, the same as Figure 6B of ref 9, β portion) or $T_{4n+2}G_2$ ($n = 1$, Figure 2C, portions c, and $n = 4$ in Figure 6C of ref 9, β' portion) in such a way that a substantial parallelism among the local chain axes is maintained. All *gauche* bonds have the same chirality (they all are G+ or G−).[25] Also, corresponding to the last regions, a bidimensional unit cell with the axes mutually orthogonal, coinciding with a_o and b_o unit cell axes of the orthorhombic structural model of form II, may be drawn. Still, the chains indicated by the thick and the thin lines are displaced by $^1/_2b_o$ with respect to each other, resulting in a centering of the bidimensional unit cell as in form II of s-PP. It is evident that the local packing mode in the defective zones of Figure 2B,C is very close to that of form IV of s-PP (Figure 2D). These defects are trapped in planes and form the "kink bands". The model structures of Figure 2B (as well as of Figure 6C of ref 9) has the property that the crystal portions including the defective regions have the atoms exactly in the same positions, as would be expected in absence of the defect,

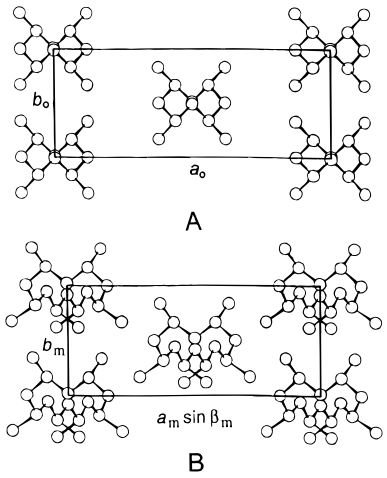

Figure 3. Orthorhombic structural model of form II, for the space group $C222_1$ (A) compared with the monoclinic structural model of form IV for the space group $C2$ (A) in projections perpendicular to the chain axis (B). For the orthorhombic model of form II $a_o = 14.50$ Å, $b_o = 5.60$ Å, and $c_o = 7.40$ Å; for the monoclinic model of form IV $a_m = 14.17$ Å, $b_m = 5.72$ Å, $c_m = 11.6$ Å, and $\beta_m = 108.8°$.

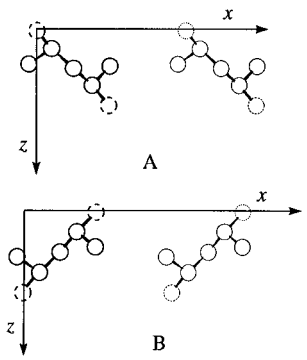

Figure 4. The asymmetric units for the slices A and B (see the text) in the *a-c* projection. The units drawn with thin and bold lines are at 0 and $^1/_2$ along *b* (perpendicular to the plane of drawing). The dashed atoms have occupation factors equal to $^1/_2$.

and the length of the defective region corresponds exactly to $2c_o$ ($3c_o$ for the defect of Figure6 C of ref 9, c_o = 7.40 Å). The model structures of Figure 2C, instead, imply a relative shift of the portions of the crystals across the defect of $^1/_4a_o$, whereas the lengths of the defects in the direction parallel to the TTGG helical axis correspond to $^3/_2c_o$. Likewise conformational sequences in the defective region of the kind $T_{4n+2}G_2$, with $n = 2$ and 3, would imply a relative shift of the portions of the crystal across the defect of $^1/_2a_o$ and $^3/_4a_o$, respectively, their lengths in the direction parallel to the axis of the TTGG helices being $2c_o$ and $^5/_2c_o$, respectively.

It is worth noting that in ref 18 it was already reported that many conformations expressed by the general formula (corresponding to a generalization of the (−TTGG−) helical conformation) ...$T_{2(2n+1)}G_2T_{2(2n'+1)}$-$G_2T_{2(2n''+1)}G_2$... might be feasible for syndiotactic polymers. In ref 18 it was reported to this last purpose "... A variety of energetically feasible conformations can be thus generated, ignoring whether or not the polymer chains are crystallizable...". In this paper indications are provided that all the chains with whatever conformation of the kind indicated can crystallize in concert (locally the chains would be all equal). The disordered model structures of Figure 2B, C (as well as of Figure 6C in ref 9) provide particular examples. They also represent a possible description of the "rigid structures placed at the interfaces of the crystallites and within strained or disordered area of the crystallites themselves" postulated by Sozzani et al. in ref 17, in order to explain the extra resonances in the solid state ^{13}C-NMR CP MAS spectra of s-PP samples of the kind examined here.

In this context it is useful to define as the "structural slice" (or more simply "slice") a portion of the crystal delimited by two parallel planes, with the crystal itself cut perpendicularly to a crystallographic plane or direction. Within the slices it is possible to identify a motif repeating regularly in two dimensions. If the dimensions of these slices are imagined to be infinite, the slices would properly correspond to a bidimensional crystal. The crystal may be described, as a consequence, in terms of a sequence of slices following each other according to suitable translation vectors.

For the ordered and disordered model structures comprising any kind of defect given by the general formula ...$T_{4n+2}G_2T_{4n'+2}$... randomly nested in an otherwise ordered portion of crystal with chains in TTGG helical conformation, we found it convenient to identify two kinds of slices, named A and B, whose asymmetric unit, drawn in Figure 4, repeats according to two perpendicular translation vectors $\mathbf{a}_o$ and $\mathbf{b}_o$. The origin of the system coordinates of the slices and the coordinates of the asymmetric units of the atoms in the slices are so chosen that the following points are true.

(1) The regular alternation of slices A and B through the translation vector $\mathbf{t} = \mathbf{c}_o/2$ gives rise to the regular TTGG helix conformation.

(2) The sequence AA or BB through the translation vectors $\mathbf{t}' = \mathbf{a}_o/4 + \mathbf{c}_o/2$ and $\mathbf{t}'' = -\mathbf{a}_o/4 + \mathbf{c}_o/2$, respectively, originates a *trans*-planar sequence of six dihedral angles. Hence, long *trans* planar sequences of the series T_{4n+2} may be generated by the juxtaposition of $n + 1$ like slices i.e. $(A)_{n+1}$ or $(B)_{n+1}$.

(3) The juxtaposition of an unlike slice after a sequence of the kind $(A)_{n+1}$ or $(B)_{n+1}$ through the translation vector $\mathbf{t} = \mathbf{c}_o/2$ bends the chain, giving rise at the junction to a G_2 conformational sequence.

For instance the model structure with chains in the conformational sequence ...$T_2G_2T_6G_2T_{10}G_2T_{18}G_2$... is given by piling through the proper translation vectors the slices ...ABBAAABBBBBA...; the limit-ordered structural model of form IV, instead, is given by the regular alternation of the slices, $(AAB)_n$ or $(BBA)_n$ providing that the two pieces of chain in the asymmetric units of Figure 3 are placed at the proper distance and that the asymmetric unit repeats according to the two perpendicular translation vectors $\mathbf{a}_m$ and $\mathbf{b}_m$.

Since kink bands may be regarded as "stacking faults" cutting the chain axes, but preserving a substantial parallelism of the chain, in this paper we calculate the X-ray diffraction profiles of various disordered model structures involving kink bands, with the methods developed for the stacking faults.[26]

Calculation Method

In the considered model structures the disorder develops along one direction only (*z*). The square modulus of the structure factor (*I*), to be compared with the experimental X-ray diffraction intensity (I_o), is calculated following Allegra in ref 26a,b.

The size distribution of the structural slices is described by Bernoulli-type statistics in two dimensions (see ref 26b). The general slice consists of identical rows of N_a unit cells along the axis *a* and identical rows of N_b unit cells along *b*, and its probability of existence is

$$p_L(N_a,N_b) = \alpha\beta(1-\alpha)^{N_a-1}(1-\beta)^{N_b-1} \qquad (1)$$

with α and β being the respective probabilities that any row along *a* and *b* lies on the slice edge. As far as the statistical correlation between different slices is concerned, the following possible events are considered: (1) the general slice is followed by no other slice along *c*, i.e. it is a terminal slice, with probability γ; (2) the general slice is followed by another slice with probability $(1-\gamma)p_{ij}$, with p_{ij} the conditional probability that the given slice of kind *i* is followed by a slice of kind *j* along *z*. As a consequence a/α, b/β, and c/γ would correspond to the average dimensions of the crystallites along the three directions *a*, *b*, and *c*, respectively. Following the method given by Allegra,[26] the calculation of the square modulus of the structure factor, *I*, is given by

$$I = D^2\{\Psi(\alpha,\mathbf{s}\cdot\mathbf{a})\Psi(\beta,\mathbf{s}\cdot\mathbf{b})\mathbf{FB}[-\mathbf{E}_n + (\mathbf{E}_n - \mathbf{M})^{-1} + (\mathbf{E}_n - \mathbf{M}^*)^{-1}]\mathbf{F}^{*\mathbf{T}}\} \qquad (2)$$

where *D* is the Debye factor (taken as in ref 22, with B = 8 Å^2, which is a quite normal value for semicrystalline polymers,[27]) **s** is the reciprocal scattering

$$\mathbf{M} = (1-\gamma) \times \begin{vmatrix} p_{11}\exp(-2\pi i \mathbf{t}_{11}\cdot\mathbf{s}) & p_{12}\exp(-2\pi i \mathbf{t}_{12}\cdot\mathbf{s}) & p_{13}\exp(-2\pi i \mathbf{t}_{13}\cdot\mathbf{s}) & \dots \\ p_{21}\exp(-2\pi i \mathbf{t}_{21}\cdot\mathbf{s}) & p_{22}\exp(-2\pi i \mathbf{t}_{22}\cdot\mathbf{s}) & \dots & \dots \\ p_{31}\exp(-2\pi i \mathbf{t}_{31}\cdot\mathbf{s}) & \dots & \dots & \dots \\ \dots & \dots & \dots & p_{nm}\exp(-2\pi i \mathbf{t}_{nn}\cdot\mathbf{s}) \end{vmatrix} \quad (3)$$

vector $2(\sin\vartheta)/\lambda$, $\mathbf{E}_n$ is the unit matrix of order n, n is the number of slices to be mixed, $\mathbf{F}$ is the row vector whose elements are the structure factors of the unit cells belonging to the various kind of slices, $\mathbf{F}^{*\mathbf{T}}$ is the column vector of the corresponding complex conjugates, and $\mathbf{B}$ is the $n \times n$ diagonal matrix whose elements are the *a priori* probabilities of occurrence of the various slices. $\mathbf{M}$ is the $n \times n$ matrix (eq 3).

$\mathbf{M}^*$ is the corresponding complex conjugate and p_{ij} are the conditional probabilities that a given slice of kind i is immediately followed by a slice of kind j, through the translation vector $\mathbf{t}_{ij}$.

The function $\Psi(\alpha,\mathbf{s}\cdot\mathbf{a})$ (and *mutatis mutandis* the function $\Psi(\beta,\mathbf{s}\cdot\mathbf{b})$) correspond to:[19b]

$$\Psi(\alpha,\mathbf{s}\cdot\mathbf{a}) = \frac{\alpha(2-\alpha)}{\alpha^2 + 2(1-\alpha)(1-\cos 2\pi\,\mathbf{s}\cdot\mathbf{a})} \quad (4)$$

Within this scheme, identifying the slices 1 and 2 with the slices A and B, respectively, the matrix $\mathbf{M}$ may be written as

$$\mathbf{M} = (1-\gamma)\begin{vmatrix} (1-p)\exp(-2\pi i \mathbf{t}'\cdot\mathbf{s}) & p\exp(-2\pi i \mathbf{t}\cdot\mathbf{s}) \\ p\exp(-2\pi i \mathbf{t}\cdot\mathbf{s}) & (1-p)\exp(-2\pi i \mathbf{t}''\cdot\mathbf{s}) \end{vmatrix} \quad (5)$$

where p and $(1-p)$ are the probabilities that unlike and like slices follow one each other, respectively. We recall that $p = 1$ corresponds to built up crystals with chains in a fully helical (TTGG) conformation, whereas $p = 0$ would correspond to chains in a all-*trans* planar conformation.

For the limit-ordered structural model of form II as well as for the disordered model structures, the $a-b$ unit cell dimensions are assumed to be equal to $a_o = 14.5$ Å, $b_o = 5.6$ Å;[22,24] for the limit-ordered monoclinic structural model of form IV the $a-b$ unit cell dimensions are taken as $a_m = 14.17$ Å, $b_m = 5.72$ Å,[20] instead. In the calculations the average dimensions of the crystallites were optimized in order to mimic at the best the half-height width and the diffuse scattering height subtending the Bragg peaks in the experimental profile. This leads to set $a/\alpha \approx b/\beta \approx c/\gamma = 45$ Å.

Results and Discussion

The calculated X-ray diffraction patterns for bundles of chains packed according to the limit-ordered structural models of form II and form IV of s-PP are reported in parts A and B of Figure 5, respectively. The most intense reflections are located at $2\theta = 12.2$, 17.1, 20.8, 24.4, and 27.3° for form II and at $2\theta = 13.1$, 17.4, 19.6, and 21.9° and correspondingly to an unresolved doublet at $2\theta = 24.5$ and 25.1° for form IV. It is apparent that the calculated X-ray diffraction pattern for the limit-ordered structure of form II (Figure 5A), presents the four most intense reflections in the same positions as the experimental pattern (Figure 1B), although in the calculated pattern the intensity ratios among the reflections at $2\theta = 17.0°$ and those at 12.2, 20.5, and 27.3° are higher than the experimental ones. The positions of the most intense peaks in the calculated pattern for the limit-ordered structure of form IV (Figure 5B) instead, are not in agreement with those in the experimental pattern (Figure 1B). On the basis of this analysis, in agreement with the information coming from our previous ^{13}C NMR CP MAS investigation,[9,10] it is hence possible to exclude that our sample is prevailingly in form IV, although the presence of some crystallites in this latter form in a small amount cannot be excluded.

Figure 6 shows the calculated diffraction patterns for disordered model structures comprising the slices named A and B of Figure 3, for $p = 0.9$, 0.85, 0.8, and 0.7 (Figure 6A−D, respectively). It is evident that inclusion of *trans*-planar sequences in the fully helical $C222_1$ limit-ordered structural model, breaking the symmetry locally, reduces mainly the intensity of the diffraction peaks located at $2\theta = 12.2$, 20.8, and 27.3° with respect to the diffraction intensity of the peak at $2\theta = 17.1°$. A good agreement with the experimental diffraction profile is obtained, when *trans* planar sequences are included in an otherwise fully helical TTGG structure, in the amount of ≈20% ($p = 0.85-0.80$; cf. Figure 1B with Figure 6B,C). Inclusion of a higher amount of such defects, would lower the intensities of the reflections at $2\theta = 12.2$ and 20.8°, with respect to the intensity of the reflection at $2\theta = 17.1°$, too much, which is not in agreement with the experimental pattern (cf. Figure 6D and Figure 1B). We notice that we cannot exclude that the pattern of Figure 1B may also originate from a mixture of crystallites in the limit-ordered form II and form IV, together with crystallites including different amounts of disorder (for instance also crystallites with $p \le 0.7$) for a total amount of T_{4n+2} sequences equal to ≈20%. The inclusion of ≈20% of T_{4n+2} sequences, mostly T_6, corresponds to the presence of one defect every 20−30 monomeric units (1−1.5 defects for each crystallite on average); each T_{4n+2} sequence (with $n > 0$) implies the presence of two methylene groups in the TT.TG conformational environment (where the dot stands for the CH_2 position). It follows that 15−20% of these defects corresponds to the presence of ≈10% of the total number of CH_2 in the TT.TG conformational environment, in good agreement with the quantitative

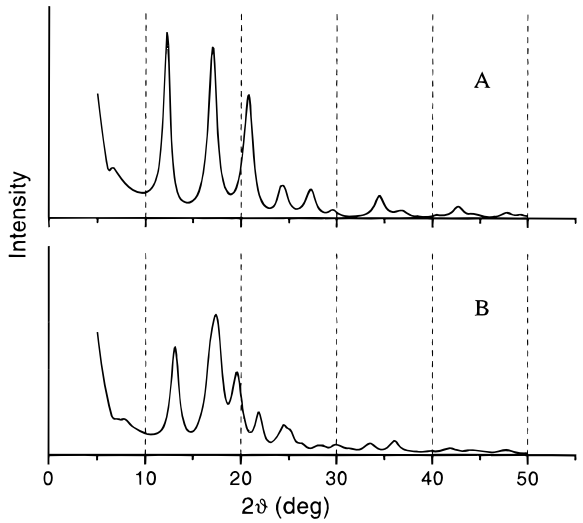

Figure 5. Calculated X-ray powder diffraction profiles for the limit-ordered structural models as proposed for form II (space group $C222_1$) (A) and form IV (space group $C2$) (B) of s-PP. $a/\alpha = b/\beta = c/\gamma = 45$ Å.

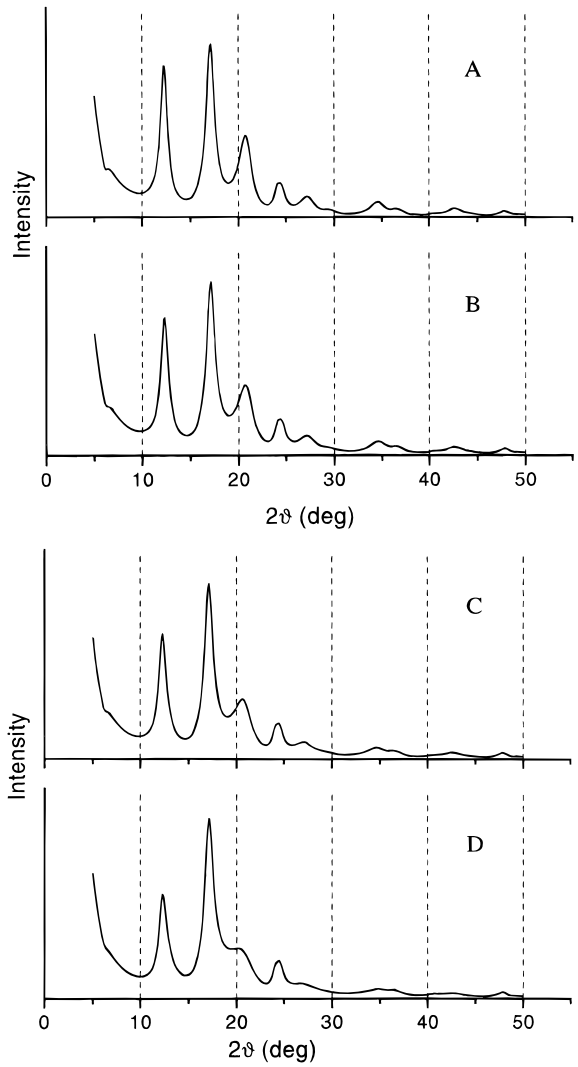

Figure 6. Calculated X-ray powder diffraction profile for a disordered model structure with $p = 0.9$ (A), $p = 0.85$ (B), $p = 0.8$ (C), and $p = 0.7$ (D). $a/\alpha = b/\beta = c/\gamma = 45$ Å.

estimations based on the solid state ^{13}C NMR CP MAS data.[9]

Concluding Remarks

In this paper the presence of local conformational disorder in some powder specimens of s-PP having structural features very close to those of form II is examined. This disorder consists of the presence of long portions of chains in the *trans* planar conformation embedded between portions of crystal with chains in the more stable TTGG conformation, forming kink bands. In this paper we have shown that such a disorder not only explains the solid state ^{13}C NMR CP MAS spectra of the samples under examination but also produces X-ray diffraction profiles in good agreement with the experimental pattern. The presence of kink bands, breaking locally the high symmetry of $C222_1$ space group as proposed for the limit-ordered model structure of s-PP in form II, mainly influences the intensity of the Bragg reflections at $2\theta = 12.2$ (Miller indices (200)), at $2\theta = 20.8°$ (Miller indices (111)), and at $2\theta = 27.3°$ (Miller indices (202) + (311) + (401)) which in the limit-ordered form II would be too high with respect to the experimental case. The agreement with the experimental pattern may be obtained with the introduction of 15−20% *trans* planar sequences in an otherwise ordered structure with chains in a TTGG fully helical conformation. This agreement is obtained, for instance, for small crystallites of average dimensions around 45 Å in the *a*, *b*, and *c* directions, comprising short $T_{2(2n+1)}$ sequences, mostly T_6, one every 20−30 monomeric units.

Acknowledgment. The authors thank Dr. Maurizio Galimberti of "Montell" of Ferrara for providing the examined sample. This work was supported by the Ministero dell'Università e della Ricerca Scientifica e Tecnologica (Italy) and by the Consiglio Nazionale delle Ricerche.

References and Notes

(1) Wunderlich, B. *Macromolecular Physics*; Accademic Press: New York, 1973; Vol. 1.
(2) Speerschneider, G. J.; Li, C. H. *J. Appl. Phys.* **1962**, *33*, 1871−1883.
(3) O'Leary, K.; Geil, P. H. *J. Appl. Phys.* **1967**, *38*, 4169−4181.
(4) Wunderlich, B.; Melillo, L. *Makromol. Chem.* **1968**, *118*, 250−264.
(5) Zaukelies, D. A. *J. Appl. Phys.* **1962**, *33*, 2797−2803.
(6) Buchdahl, R.; Zaukelies, D. A. *Angew. Chem.* **1962**, *74*, 569−573.
(7) Takahashi, Y.; Tadokoro, H., Odajima, A. *Macromolecules* **1990**, *13*, 1318−1320.
(8) Takahashi, Y.; Tadokoro, H. *Macromolecules* **1980**, *13*, 1316−1317.
(9) Auriemma, F.; Born, R.; Spiess, H. W.; De Rosa, C.; Corradini, P. *Macromolecules* **1995**, *28*, 6902−6910.
(10) Auriemma, F.; Lewis, R. H.; Spiess, H. W.; De Rosa, C. *Macromol. Chem. Phys.* **1995**, *196*, 4011−4024.
(11) De Rosa, C.; Auriemma, F.; Corradini, P. *Macromolecules* **1996**, *29*, 7452−7459.
(12) Lotz, B.; Lovinger, A. J.; Cais, R. E. *Macromolecules* **1988**, *21*, 2375.
(13) Lovinger, A. J.; Lotz, B.; Davis, P. D. *Polymer* **1990**, *31*, 2253.
(14) Lovinger, A. J.; Davis, D. D.; Lotz, B. *Macromolecules* **1991**, *24*, 552.
(15) Lovinger, A. J.; Lotz, B.; Davis, D. D.; Padden, F. J. *Macromolecules* **1993**, *26*, 3494.
(16) De Rosa, C.; Auriemma, F., Vinti, V. *Macromolecules* **1997**, *30*, 4137.
(17) Sozzani, P.; Simonutti, R.; Galimberti, M. *Macromolecules* **1993**, *26*, 5782−5789.
(18) Chatani, Y.; Muruyama, Y.; Asanuma, T.; Shiomura, T. *J. Polym. Sci., Polym. Phys.* **1991**, *29*, 1649−1652.
(19) Sozzani, P.; Simonutti, R.; Comotti, A. *Magn. Reson. Chem.* **1994**, *32*, S45−S52.
(20) Auriemma, F.; De Rosa, C.; Ruiz de Ballesteros O., Vinti V., Corradini, P. Submitted to *J. Polym. Sci.: Pol. Phys. ed.*
(21) Auriemma, F.; De Rosa, C.; Corradini, P. *Macromolecules* **1993**, *26*, 5719
(22) De Rosa C.; Corradini, P. *Macromolecules* **1993**, *26*, 5711−5718.
(23) Balbontin, G.; Dainelli,D; Galimberti, M. ; Paganetto, G. *Macromol. Chem.* **1992**, *193*, 693−703.
(24) Corradini, P.; Natta, G.; Ganis, P.; Temussi, P. A. *J. Polym. Sci., Part C* **1967**, *16*, 2477−2484.
(25) Following the definition given by Corradini in (*The Stereochemistry of Macromolecules*; *Part III*; Ketley A. D. Ed.; Marcel Dekker Inc.: New York, 1968), it is useful to distinguish from a configurational viewpoint as (+) or (−) the bonds of the chain which are adjacent to the carbon atoms constituting the stereoisomeric centers. We recall that, in vinyl polymers, the (+) bonds tend to assume G+ or T conformations whereas (−) bonds tend to assume G− or T conformations. Syndiotactic vinyl polymers correspond to the sequence of signs ...(+)(+)(−)(−)(+)(+)... Since in the modeled structures the *trans*-planar sequences comprise $4n + 2$ bonds, all *gauche* bonds are always of the same chirality.
(26) (a) Allegra, G. *Nuovo Cimento* **1962**, *23*, 502−515. (b) Allegra, G.; Bassi, I. W. *Gazz. Chim. Ital.* **1980**, *110*, 437−442.
(27) Tadokoro, H. *Structure of Crystalline Polymers*; John Wiley & Sons; New York: 1979.

MA970284G